Nuclear Instruments and Methods in Physics Research A 795 (2015) 32–38

Contents lists available at ScienceDirect

Nuclear Instruments and Methods in Physics Research A

journal homepage: www.elsevier.com/locate/nima

On the interpretation of current–voltage curves in ionization chambers using the exact solution of the Thomson problem

M.A. Ridenti [a,*], P.R. Pascholati [b], J.A.C. Gonçalves [c], C.C. Bueno [c,**]

[a] Department of Physics, Aeronautics Institute of Technology (ITA), São José dos Campos, SP 12228-900, Brazil
[b] Laboratório do Acelerador Linear, Instituto de Física da Universidade de São Paulo, Cidade Universitária, São Paulo 01303-050, SP, Brazil
[c] Instituto de Pesquisas Energéticas e Nucleares, Cidade Universitária, São Paulo 05508-000, SP, Brazil

ARTICLE INFO

Article history:
Received 6 March 2015
Received in revised form
17 April 2015
Accepted 18 May 2015
Available online 30 May 2015

Keywords:
Steady-state charge transport
Ionization chambers
Gaseous detectors

ABSTRACT

The $I-\Delta V$ characteristic curve of a well type ionization chamber irradiated with ^{192}Ir sources (0.75 Ci–120 Ci) was fitted using the exact solution of the Thomson problem. The recombination coefficient and saturation current were estimated using this new approach. The saturation current was compared with the results of the conventional method based on Boag–Wilson formula. It was verified that differences larger than 1% between both methods only occurred at activities higher than 55 Ci. We concluded that this new approach is recommended for a more accurate estimate of the saturation current when it is not possible to measure currents satisfying the condition $I/I_{sat} > 0.95$. From the calibration curve the average value of pairs of carriers created per unit volume was estimated to be equal to $\eta = 8.1 \times 10^{-3}$ cm^{-3} s^{-1} Bq^{-1} and from that value it was estimated that ~ 17 pairs were created on average per second for each decay of the source.

1. Introduction

The description of the saturation characteristics of ionization chambers operating in current mode is a very old problem in physics which dates back to 1899, when J.J. Thomson set up the general differential equation for the transport of ions between parallel plates [1]. Many authors (Mie [2], Seeliger [3], Boag and Wilson [4]), including Thomson [1], proposed approximate solutions to this problem, but it was only many years later, in 1975, that a general solution was found by Rosen and George [5] with the only additional approximation of neglecting space charges. This was the first solution that linked the current induced by the motion of charges, I, with the voltage applied to the ionization chamber, ΔV, and provided an expression to the spacial distribution of charges. Nonetheless, the relation between current and applied voltage was found as an implicit formula of both variables (*i.e.* $F(I, \Delta V) = 0$), which makes the procedure of data fitting by the least squares method infeasible. Recently, Chabod [6] found a way to write ΔV explicitly as a function of I (*i.e.* $\Delta V = f(I)$). With this last achievement it is now possible to fit the experimental current–voltage curve of an ionization chamber using the exact solution to the Thomson problem as long as some theoretical assumptions are met. Furthermore, as far as the authors are concerned, there is still no published experimental work that applies this new approach in the analysis of current–voltage curves.

In this work, the experimental current–voltage (I–ΔV) curves of a well type ionization chamber irradiated with very intense ^{192}Ir sources with activities ranging from few curies to approximately one hundred curie were fitted using the analytical formula proposed by Chabod. This formula can be translated into a fitting function with only two parameters, which can be related with all the relevant physical variables of the problem: the saturation current I_{sat}, the recombination coefficient k, the rate of electron–ion pair formation per unit volume N, the electron and ion mobilities μ_e and μ_a, respectively, and the electrodes separation distance d. As previously stressed by Chabod, this fitting procedure paves the way for many interesting applications, such as the measurement of the recombination coefficient k, the determination of the fraction of charges that escape recombination, the estimate of the ionization chamber efficiency and the extrapolation of the saturation current value using parts of saturation curves.

A typical problem in the dosimetry of very intense radioactive sources is the determination of the saturation current required in calibration procedures of ionization chambers used as dose and activity meters. In these cases, very high applied voltages are

* Corresponding author.
** Principal corresponding author.
E-mail addresses: aridenti@ita.br (M.A. Ridenti), ccbueno@ipen.br (C.C. Bueno).

http://dx.doi.org/10.1016/j.nima.2015.05.042

needed to achieve the saturation plateau. In practice, such high voltages can produce sparks and hence should be avoided. In this case, the saturation current must be extrapolated from the recombination region of the I–ΔV curve. Old theories addressed this problem, but they were valid only when $I/I_{sat} > 95\%$. In many cases, the measured I–ΔV curve does not satisfy this condition and only a valid fit of the recombination region would give a good estimate of the saturation current. As an example of application, it will be shown how a calibration procedure that uses the traditional extrapolation approach (*e.g.* Boag–Wilson formula [4]) to determine the saturation current differs from a calibration procedure that uses the exact solution. Using this method, it can be shown that the upper limit of the activity range of ionization chambers may be extended to higher values.

1.1. The Thomson problem

The Thomson problem is basically the set of differential equations that describe macroscopically the transport of positive and negative charge carriers through a gaseous medium subject to a static electric field. It is assumed that: (i) the diffusion contribution to the charge velocities is negligible in comparison with the electric field contribution; (ii) there is no charge multiplication by electron impact ionization or any other ionization process; (iii) there is only two types of charge carriers: one of them is negative and is always an electron (n_e designates the electron density); the other one is positive and is always a singly ionized atom (n_a designates the positive ion density); (iv) the charge recombination occurs by a mechanism whose rate may be written as kn_an_e; (v) the pair creation is caused only by the ionizing radiation and its rate of formation per unit volume, N, is considered to be constant all over the active volume of the detector chamber; (vi) the charge velocities are proportional to the magnitude of the field, the proportionality constants being the mobilities μ_e and μ_a. Considering that the problem has planar symmetry (cf. Fig. 1) and that all the above-mentioned hypotheses are valid, plus the proper boundary conditions, the physical variables n_e, n_a and E can be coupled through the continuity equations of the positive and negative carriers and the Poisson equation

$$\begin{cases} -\mu_e \dfrac{\partial}{\partial z}(n_e E) = N - kn_en_a \\ \mu_a \dfrac{\partial}{\partial z}(n_a E) = N - kn_en_a \\ \dfrac{\partial}{\partial z} E = \dfrac{e}{\varepsilon_0}(n_a - n_e) \\ n_e(d) = 0, \quad n_a(0) = 0, \quad \int_0^d E(z)\,\mathrm{d}z = \Delta V \end{cases} \tag{1}$$

where e is the elementary charge and ε_0 is the vacuum permittivity. Although the above set of differential equations is apparently simple, an analytical solution to it has not been found yet.

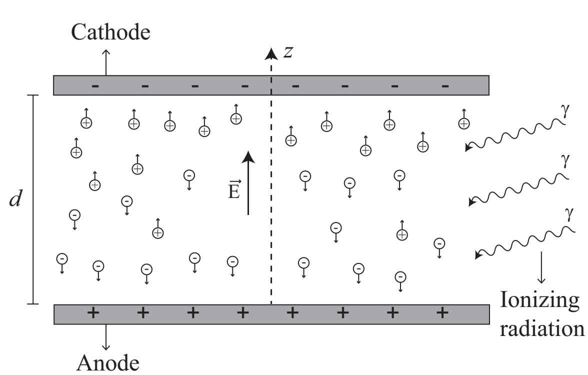

Fig. 1. Schematic view of a parallel plate ionization chamber.

Fortunately, the space charge effect may be neglected in many practical situations (*i.e.* the component of the field generated by the charged electrodes prevails over the field generated by the free carriers), and the set of equations may be simplified to

$$\begin{cases} -\mu_e E \dfrac{\partial}{\partial z} n_e = N - kn_en_a \\ \mu_a E \dfrac{\partial}{\partial z} n_a = N - kn_en_a \\ n_e(d) = 0, \quad n_a(0) = 0, \quad E = \frac{\Delta V}{d}. \end{cases} \tag{2}$$

This equation may be solved analytically to give the spacial distribution of negative and positive charges, as shown by Rosen and George [5]. The spacial distribution of electrons, for instance, is given by the following formula, which will be useful later when computing the space charge effects [6]

$$n_e(x) = \frac{kI - K\ \tan\left((K/2eS\nu_e\nu_a)(x+C)\right)}{2eSk\nu_e} \tag{3}$$

where S is the electrode surface area, $\nu_e = \mu_e E$ and $\nu_a = \mu_a E$ are the electron and positive ion drift velocities, respectively, and C is an integration constant which may be evaluated using the boundary condition $n_e(d) = 0$ and

$$K = \sqrt{4kNe^2S^2\nu_e\nu_a - k^2I^2}. \tag{4}$$

As it was shown by Chabod [6], the following law links the voltage ΔV to the current I:

$$\Delta V = \begin{cases} \Delta V_0 \times \dfrac{\sqrt{1+\sqrt{1-\eta^2\Xi(\eta)^2}}}{\Xi(\eta)} & \text{when } \eta \geq \beta, \\ \Delta V_0 \times \dfrac{\sqrt{1-\sqrt{1-\eta^2\Xi(\eta)^2}}}{\Xi(\eta)} & \text{when } \eta \leq \beta. \end{cases} \tag{5}$$

where $\beta = 2/\pi$ and

$$\begin{cases} \eta = \dfrac{I}{I_{sat}} \\ \Delta V_0 = \dfrac{d^2}{\sqrt{2}}\sqrt{\dfrac{kN}{\mu_e\mu_a}} \end{cases} \tag{6}$$

and the function $\Xi : [0,1] \to [0,\pi]$ is given by

$$\Xi\left(\frac{\sin(x)}{x}\right) = x. \tag{7}$$

No additional assumption is made as (5) may be derived only by simplification and rearrangement of the expression of the electron spacial distribution [6]. As it will be shown later, expression (5) may be set as the model function in the least squares procedure. In general, only two variables must be assigned as adjustable parameters: I_{sat} and ΔV_0.

The main goal of this work is to show that Eq. (5) can provide a good description of a real current–voltage curve as long as some assumptions are met. It will be shown in the next section that the experimental conditions are to a good degree of accuracy consistent with the theoretical hypotheses. By no coincidence the experimental data can be quite accurately fitted using (5); from the adjusted parameters valuable information may be extracted which, as mentioned before, relates with physical quantities and may be useful in many applications.

2. Materials and methods

2.1. Experimental setup

The experimental setup and results were presented in the previous paper [7]. Here only a brief description is given and the mentioned paper should be consulted for further details. The ionization chamber (Fig. 2) consisted of 15 inner collecting electrodes (radius = 6 cm), 15 mm apart, with its active volume of 2070 cm^3 filled with pure argon under a pressure of 1 bar. The detector was connected to a Keithley model 617 Programmable Electrometer, fully computer-controlled by means of specially designed software. A high DC voltage power supply (Stanford, PS300) was applied to the chamber. The detector was irradiated with sealed ^{192}Ir sources whose activities ranged from 27 GBq (0.75 Ci) up to 4.1 TBq (110 Ci). These sources were formed by adding up to 20 ^{192}Ir pellets with activities from 296 GBq (8 Ci) up to 0.63 TBq (17 Ci) each, supplied by NORDION Inc. The correction factors for self-absorption of photons within the pellets and sample holders were evaluated by Monte Carlo simulation, as described in Ref. [7], and then applied to compute the effective activity seen by the chamber.

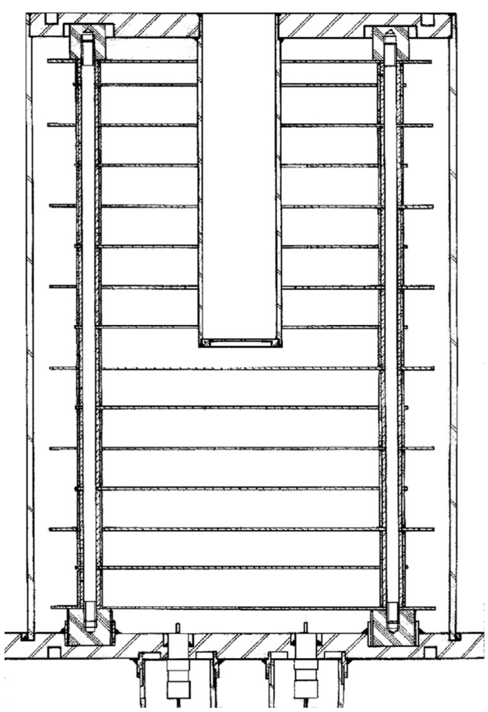

Fig. 2. Longitudinal section of the cylindrical ionization chamber with parallel electrodes.

2.2. Assumption analysis: diffusion, space-charges, transport parameters and recombination regime

2.2.1. Diffusion losses

One important assumption of the Thompson problem is that losses of charges due to diffusion to the walls are negligible. The validity of this assumption depends on the particular physical configuration of the chamber and other parameters, such as electric field and gas temperature.

Rosen and George made an estimate of the diffusion losses on their hypothetical experimental configuration [5]. They assumed that diffusion and the charge mobilities could be related by means of the Einstein relation no matter was the nature of the charge carriers. This is generally true in the case of heavy ions, but very often Einstein relation completely fails to describe the transport of electrons even at low and intermediate values of reduced electric field (defined as the electric field E divided by the gas density n, $E_{red} = E/n$). In this case, the electron diffusion coefficient and mobility should be extracted from measured data or calculated by means of a Boltzmann solver or Monte Carlo algorithm.

The average lifetime τ_D of particle against diffusion and the mean transit time τ_v due to the electric drift are given by the following expressions:

$$\tau_D = \frac{r^2}{2D_i} \tag{8}$$

$$\tau_v = \frac{d^2}{\mu_i \Delta V} \tag{9}$$

where r is the electrode radius, $i = e, a$ is the index indicating whether the quantities refer to electrons or positive ions, D_i is the diffusion coefficient and μ_i is the mobility. Table 1 shows the main physical parameters used to evaluate τ_D and τ_v and their ratios. Since argon was used as the filling gas, the positive ion mobilities were considered to be only due to the drift of Ar^+ ions and were extracted from the table of values calculated by Dalgarno [8]. Since only low reduced electric fields are being considered, no important equilibrium deviation should be present and the diffusion coefficient may be estimated using Einstein relation. In the electron case, both electron mobility and radial diffusion were calculated using a Boltzmann solver based in the standard two term expansion of the electron energy distribution function in Legendre polynomials [9].

The results are presented in Table 1, showing that diffusion losses are negligible in the case of positive ions as well as in the case of electrons. The ratio τ_v/τ_D is higher in the electron case, though not high enough to overcome the drift time. Even in the case of very low electric field, when ΔV is set to 10 V, the electron diffusion average time is only 1% of the transit time and it may only contribute as a second order effect.

It should also be mentioned that the previous analysis is valid if the assumption of no space-charges effect is also taken into account. If it was not the case, the ambipolar diffusion coefficient

Table 1
Electron (e^-) and positive ion (Ar^+) diffusion, drift velocities, diffusion and drift average times and their ratios.

ΔV (V)	E_{red} (Td)	D_e (m^2/s)	v_e (m/s)	τ_D (s)	τ_v (s)	Ratio
Electron (e^-) *component*						
10	2.7×10^{-3}	0.16	1.1×10^3	1.0×10^{-3}	1.3×10^{-5}	1.4×10^{-2}
100	2.7×10^{-2}	0.75	2.1×10^3	2.1×10^{-3}	7.1×10^{-6}	3.4×10^{-3}
1000	2.7×10^{-1}	0.37	3.7×10^3	4.2×10^{-3}	4.0×10^{-6}	9.7×10^{-4}
Positive ion (Ar^+) *component*						
10	2.7×10^{-3}	4.4×10^{-6}	0.18	353	0.48	1.4×10^{-3}
100	2.7×10^{-2}	4.4×10^{-6}	1.8	353	4.8	1.4×10^{-4}
1000	2.7×10^{-1}	4.4×10^{-6}	18	353	48	1.4×10^{-5}

should be considered instead. In the next subsection, the effect of space-charges will be discussed.

2.2.2. Space-charges

Another important assumption that should be verified is the absence of such high densities of space-charges that would eventually distort the applied field. The criterion for negligible contribution of space-charges to the electric field is that their densities should be small compared to the surface-charge on the electrodes. As shown by Von Engen [10], space-charges have to be considered only if their density exceeds $10^{14}\ \text{m}^{-3}$. Physically, it may happen if the electric field is too weak and/or the rate of pair creation is too high, making it difficult for the field to efficiently collect the charge carriers and allowing for charge build-up.

The charge density may be estimated by means of the exact solutions of the Thomson problem. For a given set of physical parameters, the maximum density may be estimated. As consistency with the assumption of no distortion by space-charges is required, then the calculated density is expected to be lower than the above-mentioned limit. In order to estimate the maximum space-charge density, it is enough to consider only the density of positive carriers, which are expected to be much higher due to their lower mobility. At the cathode vicinities the density is expected to be maximum. It is also enough to consider a maximum N value, consistent with the most intense activity source used in the experiment. This N value was chosen so that the resulting current at 1000 V was consistent with the measured one, considering a recombination rate given by the Debye equation $k = e\mu_e/\epsilon_0\epsilon_{rel}$, where ϵ_0 is the electric permittivity in vacuum and ϵ_{rel} is the relative permittivity of the medium (we shall discuss later why this expression was adopted) and all the other parameters in the same way as in the previous calculations. Fig. 3 shows the expected density profile of the positive ions at different applied voltages. In this case, if the applied voltage is lower than 200 V space-charges may distort the applied field. For this reason, the voltage interval where the model function may be legitimately adjusted to the experimental data must be carefully chosen. For instance, experimental results at lower values of ΔV may be influenced by space-charges. In this case, the corresponding data points should not be considered in the fitting procedure.

2.2.3. Transport parameters

The assumption that the transport parameters (μ_a, μ_e and k) are constant is very seldom given its deserved attention. It is actually a very restrictive constraint. If the field is uniform, the solution to the Thomson problem without space charges still holds, but the

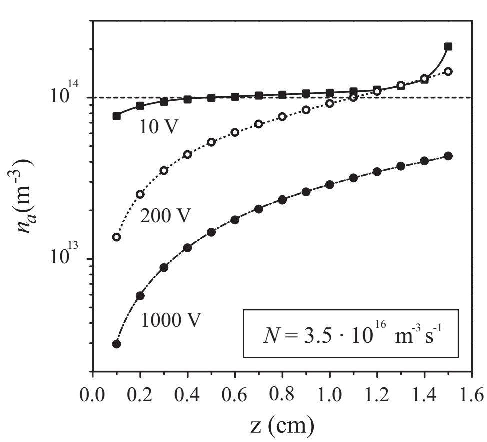

Fig. 3. Density profile of the positive carriers Ar^+ for three different applied voltages and $N = 4 \times 10^{15}\ \text{m}^{-3}\ \text{s}^{-1}$. The horizontal dashed line indicates the threshold value above which space charges may distort the applied field.

ΔV_0 would also depend on ΔV, which makes the problem of fitting the experimental I–ΔV curve much more difficult.

Rigorously, the variation of these parameters as a function of the electric field must be studied in order to verify to which extent they can be considered constant. The applied voltage ranges from 10 V to 1000 V, which corresponds to a reduced electric field interval of 0.027 Td –2.7 Td (p=1 bar, T=300 K). In this range, the mobility of the ion Ar^+ may be considered constant [11], but the electron mobility may vary from values of the order of $\mu_e \times n = 10^{26}\ \text{mV}^{-1}\ \text{s}^{-1}$ at lower fields to values near $\mu_e \times n = 10^{24}\ \text{mV}^{-1}\ \text{s}^{-1}$ at higher fields [12]. The situation gets worse in the case of the recombination coefficient, since, as far as we are concerned, no measured value of this parameter in this range of reduced electric field has ever been published. Shinsaka et al. [13] measured the recombination constant in a much lower interval of reduced electric field. They found that this parameter increases as a function of the reduced electric field until it reaches a maximum value near 1 mTd–$k = 1.3 \times 10^{-5}\ \text{cm}^3\ \text{s}^{-1}$ [13] – and then decreases. In spite of that fact, the experimental data may be fitted quite satisfactorily using constant parameters, as will be shown later. This suggests that the ratio μ_e/k is constant. According to the Debye model [14] this ratio is constant and equal to $\epsilon_0\epsilon_{rel}/e$. Rigorously, this model is known to be valid only in solid argon [13]. In gaseous argon, measurements show that the real recombination coefficients may be two orders of magnitude lower than the value predicted using the Debye expression [13]. Nonetheless, as it will be shown later, the measured $I - \Delta V$ curves are consistent with such large recombination coefficients and it does behave as if μ_e/k was a constant value. This may be explained if recombination occurs mainly on clusters of ionized atoms, as will be discussed in the next section.

2.2.4. Recombination regime

The so-called initial recombination occurs when the charge carriers recombine within the clusters or columns (which are overlapped clusters) formed in the path of the ionizing radiation. Within the cluster, the electric field and the mean electric energy may greatly differ from the volume averaged values. This type of recombination can be considered in a more general version of the Thomson formulation as proposed by Chabod [15,16] in which a spacial and time varying $N(\mathbf{r}, t)$ is considered. In the case treated here, where the gas is submitted to very high activities, the cluster distribution may be considered uniform.

The following criterion may be used to decide whether or not N may be considered uniform. The cluster or column may be described by a characteristic length b, which depends mainly on the nature of the medium and, to a lesser extent, on the nature and energy of the ionizing radiation [17]. This length can be estimated using the classical recombination theory, which yields the value of $b = 6 \times 10^{-3}\ \text{cm}^{-3}$ [17]. If this value is comparable to the mean distance between ions in the ionization chamber the assumption of the Thomson problem will be satisfied. The positive charge density in the chamber, considering the activity range and typical applied voltages of the experiments, can be estimated to be higher than $n_{inf} = 10^6\ \text{cm}^{-3}$. In the inferior limit, the mean distance between the ions is equal to $d = 10^{-2}$ cm, which is comparable to the cluster size. If the density is higher, this value will be even lower. This shows that, in the experimental conditions of this work, the assumption of constant N is valid. Recombination within the clusters of new born ionized particles is much more efficient than volume recombination – such as the recombination of ions in a plasma afterglow – and that justifies the use of the Debye equation to estimate the recombination coefficient.

2.3. Fitting procedure

In order to fit the theoretical curve to the experimental data a model function based on Eq. (5) with ΔV_0 and I_{sat} as the adjustable parameters was defined and adjusted by means of a weighted least squares method. The model function is not linear in the parameters (see (5)) and the least squares algorithm known as Gauss–Levenberg–Marquardt was used to search for the best estimates of the parameters and their variances [18]. The theory determines how ΔV_0 relates with other physical constants (Eq. (6)), but one of them, the average rate of pair creation per unit volume, N, can not be known a priori without additional experiments, though it is expected to be proportional to the source activity. A code in MATLAB® was written in order to implement this algorithm and evaluate the model function, which can not be expressed in terms of elementary functions commonly defined in almost all computer languages.

The current measurements exhibited random fluctuations, whose variance was estimated evaluating the standard deviation based on a statistically significant sample (type A evaluation of uncertainty). These uncertainties were taken into account in the least squares procedure. Since the current is the dependent variable, an iterative procedure was used to project its uncertainty in the axis of the independent variable. Experimental data also have errors of type B, from manufacturers specifications, but as they are believed to influence equally all the measured values, their estimated contribution was added to the uncertainty of the I_{sat} value.

3. Results and discussion

Figs. 4–6 show the measured I–ΔV curve for radioactive sources of different activities, spanning a large interval from 2.3 Ci to 120 Ci. In the condition of very large activity (Fig. 6), data points with voltages lower than 200 V were excluded due to the possibility of space charge effects at lower fields. The fitted curves are also shown in the figures, from which it can be seen that the experimental data is very well described by the proposed model. The goodness of the fit was attested after verification that the root of the reduced chi-squared yielded expected values. Nevertheless, the residual plot showed that points are not randomly scattered. This may be attributed to the effects which were not taken into account, such as space charges and the transport parameters dependence on the field, which however seems to contribute as second order deviations.

Apart from the least-squares fitting based on the exact solution of the Thomson problem, experimental data was also fitted using the Boag–Wilson formula [4], which is the first order approximation to the exact solution [19] and yields a estimate of the saturation current that will be referred as $I_{sat}^{(0)}$. In this case, some care must be taken, since the fitting is expected to yield reliable values if only points satisfying the condition $I/I_{sat} > 95\%$ are taken into account. The saturation current was estimated by both methods and their comparison showed that the relative deviation, defined as $(I_{sat} - I_{sat}^{(0)})/I_{sat}$, was higher than 1% only if activities were higher than 55 Ci. Even in the case of the most intense radioactive source studied, with an activity of 120 Ci, the deviation was only 2%.

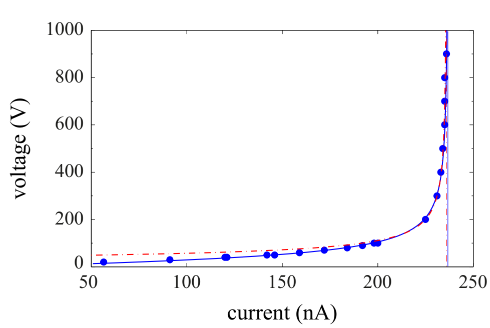

Fig. 4. Measured I–ΔV characteristic curve with a radioactive source of 2.26 Ci. The full points correspond to the experimental data and the curves represent the fitted functions using the exact solution (full line) or the first order approximation (dash-dotted line). In the last case, only points satisfying the condition $I/I_{sat} > 95\%$ were included in the fitting procedure. The vertical lines indicate the position of the I_{sat} parameter estimated using the model based on the exact solution (full line) or the model based on the first order approximation (dash-dotted line). In the first case, the resulting saturation current was $I_{sat} = 236.7$ nA and, in the second case, $I_{sat} = 236.0$ nA, yielding a relative deviation, defined as $(I_{sat} - I_{sat}^{(0)})/I_{sat}$, of 0.3%. Uncertainties are not shown, since typical values are inferior to the width of the points used to represent experimental data.

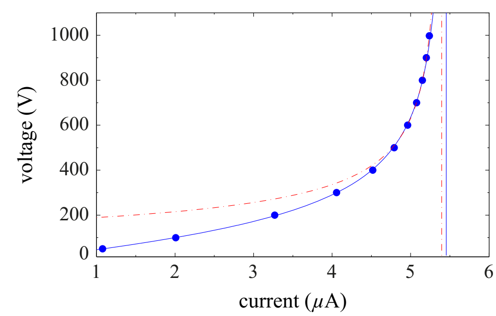

Fig. 5. Measured I–ΔV characteristic curve with a radioactive source of 55 Ci. The resulting saturation current was $I_{sat} = 5.45$ μA, in the case of the estimate based on the exact solution, and $I_{sat} = 5.40$ μA in the other case, yielding a relative deviation of 1%. The legend is the same as in Fig. 4.

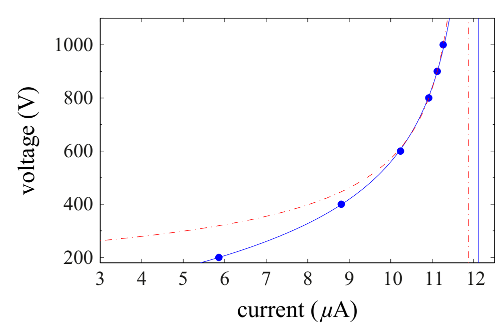

Fig. 6. Measured I–ΔV characteristic curve with a radioactive source of 120 Ci. The resulting saturation current was $I_{sat} = 12.11$ μA, in the case of the estimate based on the exact solution, and $I_{sat} = 11.88$ μA in the other case, yielding a relative deviation of 2%. The legend is the same as in Fig. 4.

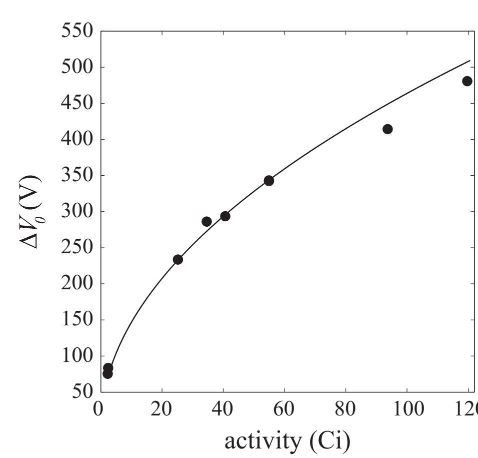

Fig. 7. ΔV_0 as a function of activity (full points) and curve (full line) that gives the best fit of the data using the model function $\Delta V_0 = a \times \sqrt{A}$, where A is the activity.

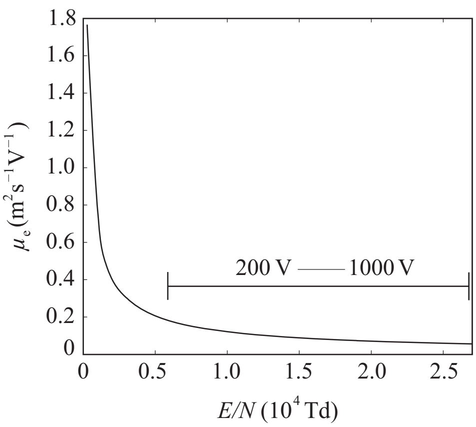

Fig. 8. Electron mobility in argon (μ_e) as a function of the reduced electron field E/N. The region that corresponds to the interval of applied voltage of 200–1000 V is highlighted.

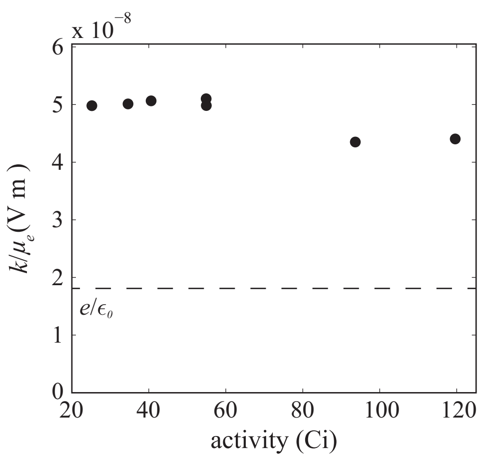

Fig. 9. k/μ_e ratio as a function of activity. The horizontal dashed line corresponds to the value from Debye's theory, $k/\mu_e \approx e/\epsilon_0$. Relative uncertainties were estimated to be $\sim$0.3% and are smaller than the point size.

The other estimated parameter, ΔV_0, may be plotted against the sources activities in order to test the model (Fig. 7). Considering that the N value is proportional to the activity, this plot should be consistent with a square root dependence of ΔV_0 with activity, as predicted by the model (Eq. (6)). In other words, this plot should be consistently described by a model function $\Delta V_0 = a \times \sqrt{A}$, where A is the activity. As mentioned in Section 2.2.3, the ratio of the parameters k and μ_e is supposed to be constant, but information on the behaviour of the mobility as a function of the applied field can be useful. Using a Boltzmann code described in the previous works which is demonstrated to give results in good agreement with swarm data [9,12], the electron mobility was computed and plotted as a function of the reduced electron field (Fig. 8). It can be seen from the graph that the electron mobility falls sharply in the low field region (10–100 V) but then it starts to fall much more slowly at higher fields. If the recombination constant is supposed to be proportional to the mobility, than it should also exhibit this behaviour.

If the ratio k/μ_e is supposed to be constant, than it can be estimated using the fitting parameters ΔV_0 and I_{sat}. From Eq. (6) and the expression relating N and I_{sat}, $N = I_{sat}/eV_{\text{eff}}$, the k/μ_e ratio may be expressed as

$$\frac{k}{\mu_e} = \frac{2}{d^4}\mu_a \Delta V_0^2 \frac{eV_{\text{eff}}}{I_{sat}} \tag{10}$$

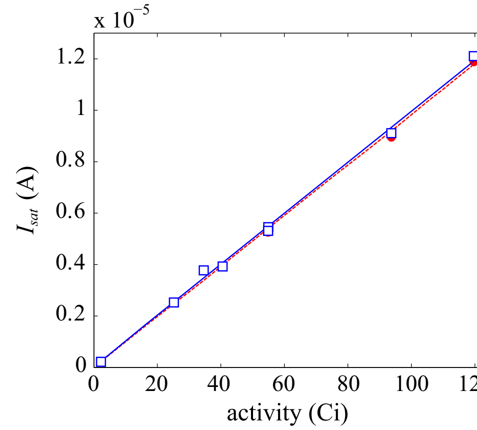

Fig. 10. Saturation current as a function of source activity. The empty square points in blue represent the estimates computed by the least square method based on the exact solution of the Thomson problem and the full curve in blue is the straight line that best fits these points. The full circle points represent the estimates computed by the least squares based on the first order approximation to the exact solution and the dashed line is the straight line that best fits these points. At lower activities, both estimates overlap at the plot scale. (For interpretation of the references to color in this figure caption, the reader is referred to the web version of this paper.)

where V_{eff} is the effective detecting volume. Fig. 9 shows the estimated k/μ_e ratios as a function of the activity. A horizontal line corresponding to the value predicted by Debye's theory is also shown. The experimental estimates were larger than the theoretical one, though values have the same order of magnitude. Values within 20 Ci and 55 Ci are approximately constant and equal to 5×10^{-8} V m. At higher values of activity, that ratio decreases to $\sim 4.4 \times 10^{-8}$ V m. This may be interpreted as a dependence of the k/μ_e ratio with activity, but the possibility of bias on the parameters estimates cannot be excluded, since fewer points were taken into account in the fitting procedure at higher activities. The observation of a higher k/μ_e ratio than the predicted one may be interpreted as a consequence of the peculiar nature of recombination within clusters, where new-born carriers are more susceptible to recombine due to its proximity to partners with opposite charge.

Another important test of linearity of the chamber is the plot of the I_{sat} parameter as a function of activity, which is shown in Fig. 10. Good linearity is observed over the entire interval of activity, showing that this chamber may be used in dosimetry of radioactive sources as high as 120 Ci. It also shows that the deviations from linearity observed in Fig. 7 are probably due to biased estimates of the parameter ΔV_0 or to a real dependence of the k/μ_e ratio with activity. As previously mentioned, the deviation between both methods of saturation current estimation is very small and their difference will be higher than 1% only at very high values of activity ($A > 55$ Ci). If better accuracy is needed for a particular application, the use of the model function based on the exact solution is recommended at high values of activity. If no current under the condition $I > 0.95 \cdot I_{sat}$ can be measured, than some care should be taken before using Boag–Wilson formula and the expression based on the exact solution should be preferred.

The average value of pairs created per unit volume and unit of activity, ξ, may be estimated from the slope α of the straight line shown in Fig. 10 through the expression

$$\xi = \frac{\alpha}{eV_{\text{eff}}}. \tag{11}$$

The resulting value is $\xi = 3.0 \times 10^8$ cm^{-3} s^{-1} Ci^{-1}. In terms of units of decays per second (Bq), the result is $\xi = 8.1 \times 10^{-2}$ cm^{-3} s^{-1} Bq^{-1}. If this value is multiplied by the chamber active volume, one may obtain an estimate of the number of pairs of charged carriers created per one ionizing event, $\xi \cdot V \approx 17$ pairs per second.

4. Conclusion

In this work the exact solution to the Thomson problem was applied for the first time in the analysis of experimental $I-\Delta V$ of an ionization chamber. A thorough analysis of the experimental and physical conditions was carried out in order to verify if the assumptions of the model were met. All the measured $I-\Delta V$ were successfully fitted using the exact solution and two fitting parameters were estimated. One of these parameters was the saturation current, which gives the maximum theoretical current, *i.e* the current that would be measured if no recombination took place. It was verified that this method offers an accurate estimate of the saturation current and that it should be used in the cases where the procedure based on Boag–Wilson formula is not valid, *e.g.* when it is not possible to measure electric current values that satisfy the relation $I > 0.95 \cdot I_{sat}$. On the other hand, it was also verified that if the latter condition is satisfied, than both estimates give equivalent results.

The second parameter, ΔV_0, which gives a measure of the voltage needed to obtain current values close to the saturation current, was also studied. This parameter depends on the carriers mobility, the recombination coefficient and the rate of pairs created by the ionizing radiation per unit volume. It could be verified that this parameter may be described as a function of the square root of the activity, as predicted by the theory. Furthermore, the ratio of the recombination coefficient to the electron mobility was found to be consistently described as a constant function of the electron field, as in the Debye equation, but with a higher proportionality constant. Debye's model of recombination is known to fail in gaseous argon, yielding overestimated values; nevertheless, it explained why it was always possible to obtain a good fit within large intervals of electric field when the electron mobility is known to vary substantially over that interval. This result was interpreted considering that the dominant recombination phenomena occurs in the clusters of ions created by the ionizing radiation.

The saturation current was experimentally shown to be proportional to the activity. From the calibration curve the average value of pairs created per unit volume and unit of activity, ξ, was estimated, yielding the value $\xi = 8.1 \times 10^{-3}$ cm^{-3} s^{-1} Bq^{-1}. For the particular chamber and activity source used during the experiments, it was estimated that ~ 17 pairs of carriers were created on average per second for each decay of the source.

Finally, we note that such a model may found applications beyond the particular problem treated here. Any physical problem involving recombination of pair of charges carriers with opposite signs may be modelled as a Thomson problem. Therefore, the same technique developed to describe the $I-\Delta V$ curve of an ionization chamber may be eventually applied to liquid and solid-state detecting devices.

Acknowledgements

This work was supported in part by the National Council for the Improvement of Higher Education (CAPES) under Contract CAPES/ITA no 005/2014. The authors are greatly indebted to Sebastien Chabod for the valuable discussions and suggestions which were crucial for the development of this work.

References

[1] J. Thomson, The London, Edinburgh, and Dublin Philosophical Magazine and Journal of Science 47 (286) (1899) 253.
[2] G. Mie, Annalen der Physik 318 (5) (1904) 857.
[3] R. Seeliger, Annalen der Physik 338 (12) (1910) 319.
[4] J. Boag, T. Wilson, British Journal of Applied Physics 3 (7) (1952) 222.
[5] R. Rosen, E. George, Physics in Medicine and Biology 20 (6) (1975) 990.
[6] S.P. Chabod, Nuclear Instruments and Methods in Physics Research Section A: Accelerators, Spectrometers, Detectors and Associated Equipment 595 (2) (2008) 419.
[7] J.A.C. Gonçalves, S. Botelho, P.R. Pascholati, M.A. Ridenti, M.M.F.R. Fraga, J.R. Camara, W.A. Calvo, C.C. Bueno, Nuclear Instruments and Methods in Physics Research Section A: Accelerators, Spectrometers, Detectors and Associated Equipment 580 (1) (2007) 222, Proceedings of the 10th International Symposium on Radiation Physics (ISRP 10).
[8] A. Dalgarno, Philosophical Transactions of the Royal Society of London, Series A, Mathematical and Physical Sciences 250 (982) (1958) 426.
[9] M.A. Ridenti, L.L. Alves, V. Guerra, J. Amorim, Plasma Sources Science and Technology 24 (3) (2015) 035002. http://dx.doi.org/10.1088/0963-0252/24/3/035002.
[10] A. von Engel, Ionized Gases, 2nd edition, Oxford University Press, London, 1965.
[11] Y.P. Raizer, Gas Discharge Physics, Primeira Edition, Springer, Berlin, Germany, 1997.
[12] M.A. Ridenti, J. Amorim, V. Guerra, A numerical solver for the homogeneous Boltzmann equation, in: Proceedings of the XI Young Researchers Meeting, Instituto de Física Gleb Wataghin, Unicamp, 2011.
[13] K. Shinsaka, M. Codama, T. Srithanratana, M. Yamamoto, Y. Hatano, The Journal of Chemical Physics 88 (12) (1988) 7529. http://dx.doi.org/10.1063/1.454317.
[14] P. Debye, Transactions of the Electrochemical Society 82 (1) (1942) 265.
[15] S.P. Chabod, Nuclear Instruments and Methods in Physics Research Section A: Accelerators, Spectrometers, Detectors and Associated Equipment 604 (3) (2009) 632. http://dx.doi.org/10.1016/j.nima.2009.03.019.
[16] S.P. Chabod, Nuclear Instruments and Methods in Physics Research Section A: Accelerators, Spectrometers, Detectors and Associated Equipment 621 (13) (2010) 316. http://dx.doi.org/10.1016/j.nima.2010.04.029.
[17] E. Kara-Michailova, D. Lea, The interpretation of ionization measurements in gases at high pressures, in: Mathematical Proceedings of the Cambridge Philosophical Society, vol. 36, Cambridge University Press, 1940, pp. 101–126.
[18] O. Helene, Método dos Mínimos Quadrados com Formalismo Matricial, 1st edition, Editora Livraria da Física, 2006.
[19] S.P. Chabod, Nuclear Instruments and Methods in Physics Research Section A 595 (2008) 419.